Journal of NUCLEAR SCIENCE and TECHNOLOGY, Vol. 48, No. 3, p. 315–321 (2011)

ARTICLE

Estimation of Heat Transfer Coefficient and Flow Characteristics on Heat Transfer Tube in Sodium-Water Reaction

Toshinori MATSUMOTO[1,*], Takashi TAKATA[1], Akira YAMAGUCHI[1], Akikazu KURIHARA[2] and Hiroyuki OHSHIMA[2]

[1]*Department of Energy and Environment Engineering, Osaka University, 2-1 Yamada-Oka, Suita, Osaka 565-0871, Japan*
[2]*Japan Atomic Energy Agency, 4002 Narita, O-arai, Higashi-Ibaraki, Ibaraki 311-1393, Japan*

(Received January 15, 2010 and accepted in revised form August 12, 2010)

In the steam generator of a sodium-cooled fast reactor, high-pressure water flows inside heat transfer tubes while liquid sodium flows on the shell side. Heat is exchanged through the tube wall. When the tube fails, water vapor leaks into the sodium stream, and a sodium-water reaction is initiated. This reaction occurs rapidly and generates a high-temperature jet. It then becomes possible for neighboring tubes to experience a secondary failure due to overheating. With regard to the secondary failure, an estimate of heat transfer from fluid to the tube is important for safety evaluation. In the present study, a numerical analysis has been carried out to determine the heat transfer coefficient from temperature data obtained in a sodium-water reaction experiment. By updating the heat transfer coefficient, an inverse problem of heat transfer has been solved in the analysis based on the result of the SWAT-1R experiment. It is found that the heat transfer coefficient fluctuates largely during the reaction. The heat transfer coefficient is affected by the flow characteristics. Hence, we characterize the flow pattern near the heat transfer tube at typical periods in the phenomenon progression.

KEYWORDS: sodium-cooled fast reactor, heat transfer tube, sodium-water reaction, overheating rupture, heat transfer coefficient, numerical simulation, inverse problem

I. Introduction

In the steam generator of a sodium-cooled fast reactor (SFR), water flows inside heat transfer tubes while the sodium flows on the shell side. When a tube fails, water vapor would leak into the sodium stream thereby initiating a sodium-water reaction (SWR).

The SWR is accompanied by erosion and corrosion in a high-temperature environment causing neighboring tubes to heat up. There is a possibility that the neighboring tubes will experience a secondary failure. The secondary failure could either come from wastage caused by erosion and corrosion or simply by tube rupture from overheating. In case of an overheating rupture, the neighboring tubes experience heat-up and the material strength deteriorates in the high-temperature environment. They then fail because of the pressure difference between the inside and outside of the tubes. For instance, in 1987, a secondary failure occurred in the superheater of the Prototype Fast Reactor (PFR) in the UK;[1] thirty-nine overheating ruptures occurred within 10 s. Therefore, the prediction of an overheating rupture in the SWR is required for the safety evaluation of the SFR steam generator (SG). From the viewpoint of the overheating rupture assessment, the tube temperature will be essential and thus a heat transfer coefficient (HTC) on the outermost tube surface is of importance.

In the previous works, the experimental results of the HTC for the SWR have been summarized based on a fluid temperature near the tube.[2] Then, a conservative value is assumed to evaluate the probability of the overheating rupture. Since flow characteristics that strongly affect the HTC were not taken into consideration in the previous works, it is apparent that the summarized data has a wide variance. The motivation of the present study is to evaluate a more accurate value of the HTC so that one achieves a best estimation of the possibility of the overheating rupture.

With regard to the experimental data, the SWAT-1R experiment was conducted by the Japan Atomic Energy Agency (JAEA)[3] to measure a temperature distribution and to estimate the HTC during the SWR. In this paper, the transient behavior of the HTC between the tube and fluid near the SWR region has been analyzed numerically by solving an inverse problem of one-dimensional thermal conductivity using the experimental data from SWAT-1R as a boundary condition. Furthermore, the flow characteristics near the SWR region have been discussed based on the magnitude of the HTC and its transient behavior.

*Corresponding author, E-mail: matsumoto_t@qe.see.eng.osaka-u.ac.jp

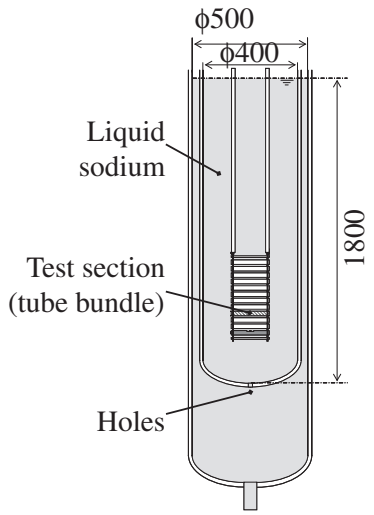

Fig. 1 SWAT-1R test vessel

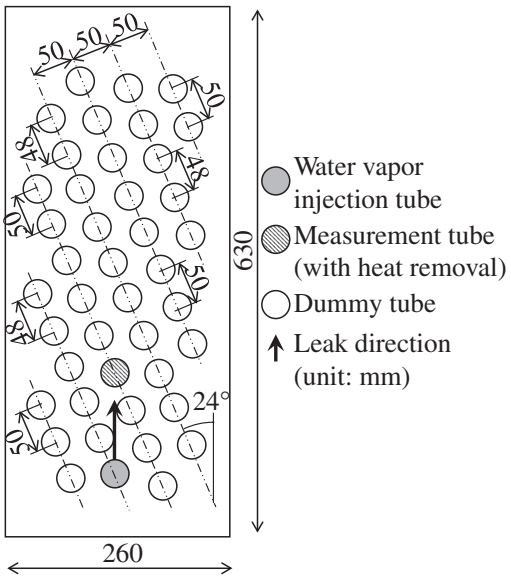

Fig. 2 Test section of SWAT-1R

II. SWAT-1R Experiment

Let us discuss the SWAT-1R experiment[3] briefly. **Figure 1** shows the schematic of the SWAT-1R test vessel. The test vessel consists of double vessels filled with stagnant liquid sodium. At the bottom of the inner vessel, there are several holes through which liquid sodium can flow to/from the outer vessel during the experiment. The test section is immersed in liquid sodium inside the inner vessel. As shown in **Fig. 2**, the test section consists of 43 dummy tubes to simulate the heat transfer tubes in the steam generator. These tubes are made of 2-1/4Cr-1Mo steel and are 31.8 mm in outer diameter and 3.8 mm in thickness.

One of tubes from which water vapor is injected into the liquid sodium is placed at the bottom of the test vessel and is labeled as "water vapor injection tube" in Fig. 2. The initial pressure and temperature of liquid sodium in the test section are set to be around 0.2 MPa and 470°C, respectively. Pressure and temperature conditions of the water vapor are set at 16.8 MPa and 350°C, respectively. The water vapor was expelled vertically upward for 30 s from the leakage nozzle that is 5.8 mm in diameter and is located at the top of the injection tube. The average leakage rate was set to 0.15–0.2 kg/s, which is categorized as "intermediate leakage."[4]

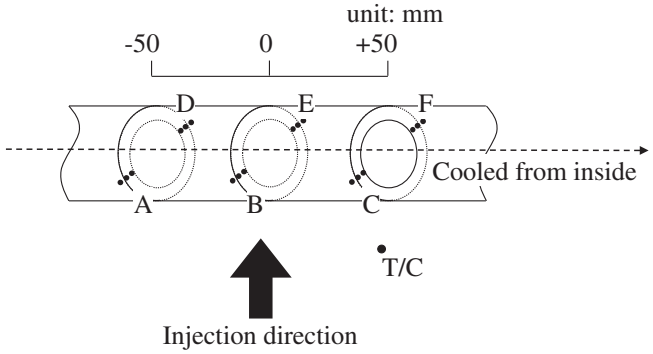

Fig. 3 Measurement tube

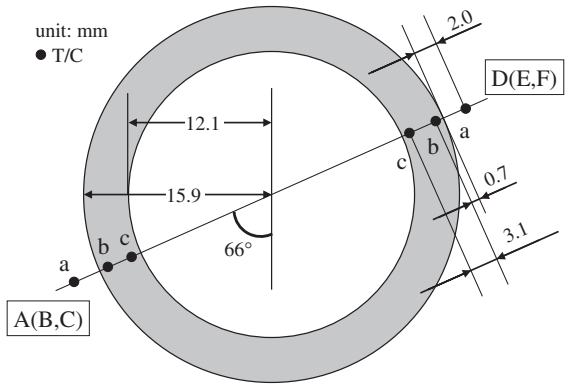

Fig. 4 Position of T/C

The temperature measurement tube was situated approximately 100 mm above the leakage nozzle (the hatched line tube in Fig. 2). Thermocouples (T/Cs) were placed at three axial locations, as shown in **Fig. 3**. Locations B and E are placed just above the leakage nozzle. Locations A, D, C, and F are set 50 mm away from the center position. **Figure 4** shows the detailed arrangement of the T/Cs. Three T/Cs were embedded in each location. One is placed in the liquid sodium 2 mm away from the tube surface (Point a). The others are embedded at different depths of the tube wall (0.7 mm (Point b) and 3.1 mm (Point c) from the outer surface). In the experiment, liquid sodium was used as a coolant inside the measurement tube. The flow rate of the liquid sodium was determined so as to achieve the same magnitude of heat removal as in the actual situation (water and/or water vapor flow).

III. Numerical Method

The temperature of the heat transfer tube is computed by solving a one-dimensional heat conduction equation in the cylindrical coordinates system. The governing equation is described as

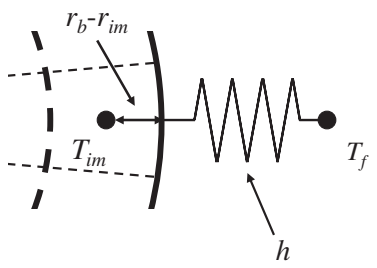

Fig. 5 Heat transfer coefficient

$$\rho C_p \frac{\partial T}{\partial t} = \frac{1}{r}\frac{\partial}{\partial r}\left(r\lambda \frac{\partial T}{\partial r}\right), \tag{1}$$

where λ, ρ, and C_p are the thermal conductivity, density, and specific heat, respectively. T, r, and t are the temperature, radial coordinate, and time, respectively. Equation (1) is discretized based on a control volume of each computational cell as

$$\rho C_p \frac{T_i^{n+1} - T_i^n}{\Delta t}\Delta V = -\lambda_{i-1/2}^n \frac{T_i^{n+1} - T_{i-1}^{n+1}}{r_i - r_{i-1}} A_{i-1/2} + \lambda_{i+1/2}^n \frac{T_{i+1}^{n+1} - T_i^{n+1}}{r_{i+1} - r_i} A_{i+1/2}, \tag{2}$$

where the subscripts i and $i \pm 1$ indicate the i-th and the adjoining control volumes, respectively. The superscripts n and $n+1$ mean the last and the subsequent time, respectively. Δt is the time step size. A is the surface area of the control volume. ΔV is the volume of the computational cell. The subscript $i \pm 1/2$ means the surface between control volumes. At the outermost surface of the tube, an HTC (h) is used to evaluate the heat flux between the tube and the fluid. A schematic of the outer surface is shown in **Fig. 5**. At the outermost computational cell, the governing equation of energy is discretized as follows:

$$\rho C_p \frac{T_{im}^{n+1} - T_{im}^n}{\Delta t}\Delta V = -\lambda_{im-1/2}^n \frac{T_{im}^{n+1} - T_{im-1}^{n+1}}{r_{im} - r_{im-1}} A_{im-1/2} + \frac{T_f^{n+1} - T_{im}^{n+1}}{\dfrac{r_b - r_{im}}{\lambda_{im}^n} + \dfrac{1}{h^{n+1}}} A_{im+1/2}, \tag{3}$$

where the subscript im means the outermost surface. T_f is the temperature of the fluid and r_b represents the outer tube radius. T_f is treated as fluid temperature. It is impossible to distinguish between a liquid and a fluid temperature from a single set of T/C data. Hence, a homogeneous fluid is assumed in the analysis and the overall HTC (h) is calculated. Then, the flow characteristics, especially in terms of void fraction, were investigated based on the magnitude of the HTC.

To solve Eqs. (2) and (3), one has to know the value of the HTC (h) and the boundary of the temperature. The following procedure is applied to obtain the HTC in each time step. The computational domain is defined in the region from Point c (inside of the tube) to Point a (fluid region). At each time step, the experimental results at Points a and c are used as the boundary condition. As a result, one can calculate the temperature distribution inside the tube under a certain HTC condition. In other words, the HTC can be evaluated inversely so that a tube temperature at a certain depth coincides with that in the experiment. The experimental result of Point b is chosen for the criterion. A bisection method is applied to the inverse procedure, and the Tri-Diagonal Matrix Algorithm (TDMA) is used for solving Eqs. (2) and (3). It is noted that when the temperature difference between the T/Cs becomes quite small, the solution does not converge for some steps (*i.e.*, infinite or negative HTC value). This will be attributed to the fact that the measurement inaccuracy increases in the case of a small temperature difference. In that situation, the time step size is incremented until the solutions of Eqs. (2) and (3) are obtained. This procedure implies that the time-averaged HTC is calculated during that time period.

IV. Numerical Investigation of Heat Transfer Coefficient in SWAT-1R Experiment

1. Numerical Conditions

In the computation, the time step and time duration are set to 0.05 and 65 s, respectively, which are the same as in the sampling procedure in the experiment. The time duration includes 5 s before injection, 30 s of injection, and 30 s after the end of injection.

With regard to the convergence criterion of the bisection method, 1.0×10^{-10} K is applied. The physical properties (specific heat, density, and thermal conductivity) of the tube material (2-1/4Cr-1Mo) are calculated using the empirical correlations.[5,6] It is noted that during the experiment, no data were obtained from one T/C at Location B, indicating some problem with that T/C.

2. Result of Heat Transfer Coefficient

(1) Lower Side of Measurement Tube (Locations A and C)

Figure 6 shows the transient history of the fluid temperature (experiment) and the HTC (analysis) at Location A. The HTC fluctuates for an initial 2 s from the injection, as shown in Fig. 6. Subsequently, the comparatively stable HTC continues until 5 s from the injection. During 5–18 s, the fluctuation of the HTC is higher than before, and unex-

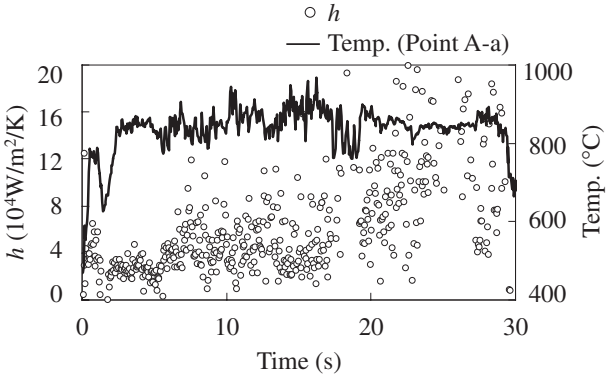

Fig. 6 Heat transfer coefficient at Location A

Table 1 Heat transfer coefficient at lower side

Location	Time (s)	Heat transfer coefficient ($W/m^2/K$)	
		Time average	Median value
A	0.0–2.0	28,000	34,000
	2.0–5.0	26,000	26,000
	5.0–18.0	95,000	42,000
	18.0–30.0	214,000	113,000
B	—	—	—
C	0.0–8.0	15,000	15,000
	8.0–17.0	27,000	25,000
	17.0–30.0	876,000	128,000

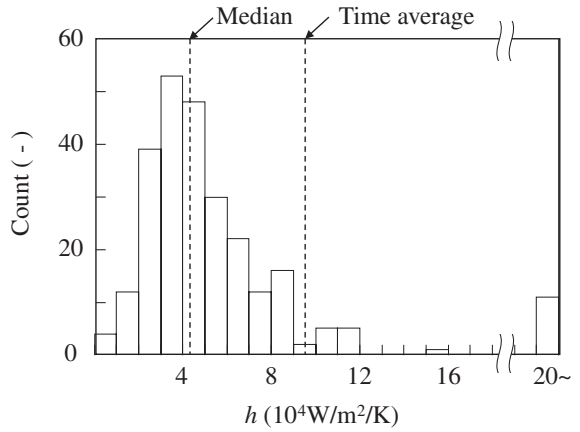

Fig. 7 Histogram of HTC during 5–18 s at Location A

plainably large values of the HTC (> 200,000 $W/m^2/K$) were intermittently calculated (*i.e.*, values beyond the range of the graph). After 18 s, the distribution of the HTC fluctuated widely. During this period, a much higher HTC was analyzed, which was over the upper limit of the graph.

Table 1 summarizes the average value of HTC at some representative time periods that are selected from the viewpoint of the HTC transient behavior. As shown in Table 1, two average values are evaluated: one is a time average value and the other is a median value. During the first 5 s, the average values are similar to each other. On the other hand, the time average value differs from that of the median after 5 s, as listed in Table 1. This is because a few extremely large values affect the time average value considerably.

Let us discuss the appropriate average value in each time period. **Figure 7** shows the histogram of the HTC during 5–18 s at Location A. The time average and median values are also indicated. The median value corresponds to the mean of the histogram excluding the extremely large values. The time history of the temperature at Point A-b has also been simulated by solving Eqs. (2) and (3) with the time average and median HTCs in Table 1. The computational results and the comparison with the experimental measurement are shown in **Fig. 8**. The result using the median value agrees with the measured history much better than that with the time average value. Hence, the median value is chosen as the representative value in each period.

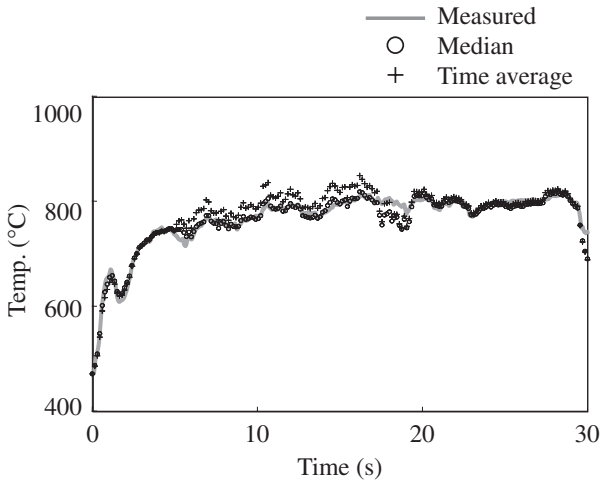

Fig. 8 Temperature history at Point A-b

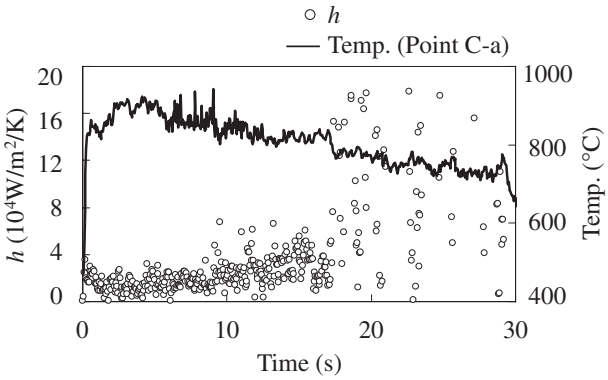

Fig. 9 Heat transfer coefficient at Location C

At Location C, a similar transient of the HTC is investigated, as shown in **Fig. 9**, although the comparatively large fluctuation does not appear at the beginning of the injection (0–2 s in Fig. 6). During 0–17 s, the fluctuation of the HTC seems to be smaller than that at Location A. After 17 s from the injection, a sudden and wide fluctuation is evaluated at Location C. Furthermore, often in this period, the analysis failed to converge (see the number of the plotted data in Figs. 6 and 9). As seen in the fluid temperature history (solid line in Fig. 9), a sudden decrease was observed in the experiment at around 17 s. As a result, a small temperature difference between the fluid and the tube was achieved, resulting in no analytical solution. It may be said that the T/C in the fluid at Location C had some trouble 17 s after the injection.

(2) Upper Side of Measurement Tube (Locations D, E, and F)

Figures 10, **11**, and **12** shows the estimated HTC and the measured fluid temperature. **Table 2** summarizes the representative value of the HTC for each period. At the upper side, similar histories of the HTC have been obtained regardless of location. The HTC in the initial 5 s fluctuated significantly. The median value of the HTC in this period is estimated to be approximately 50,000 $W/m^2/K$ at each location, as shown in Table 2. After 5 s from the injection, the HTC becomes nearly constant (Figs. 10–12). The repre-

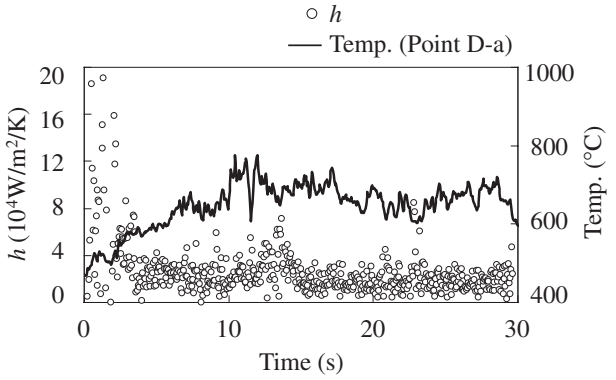

Fig. 10 Heat transfer coefficient at Location D

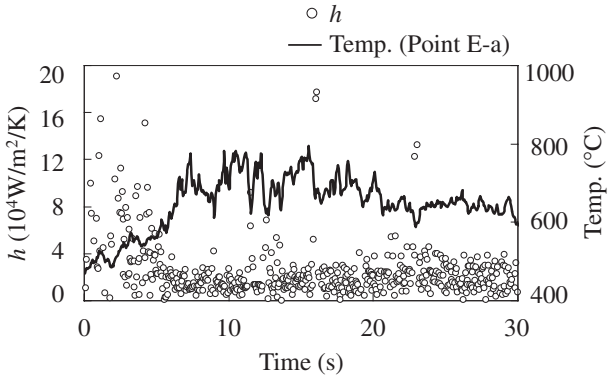

Fig. 11 Heat transfer coefficient at Location E

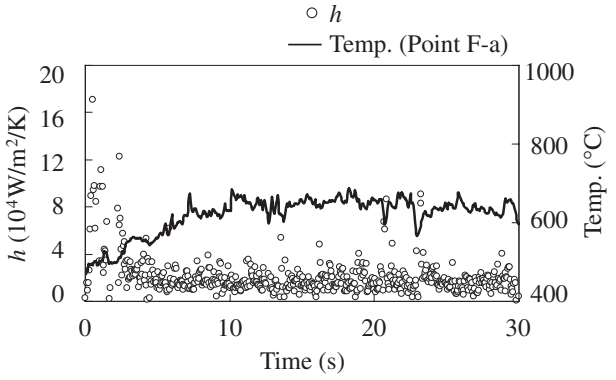

Fig. 12 Heat transfer coefficient at Location F

sentative value after 5 s is estimated to be 20,000 $W/m^2/K$ or less (Table 2). The HTC at Location D is estimated to be slightly higher than that at Location F.

3. Discussion of Flow Characteristics

As shown in Tables 1 and 2, the HTC varies quite widely throughout the SWR, which is caused by fluid characteristics, such as void fraction and velocity. For instance, an equivalent HTC is approximately 26,000 $W/m^2/K$ when the thermal conductivity of liquid sodium is only assumed between Point a and the tube surface. Moreover, the velocity of fluid (liquid or gas) should be fast because the high-pressure water vapor is rapidly expelled (at least, an acoustic velocity

Table 2 Heat transfer coefficient at upper side

Location	Time (s)	Heat transfer coefficient ($W/m^2/K$)	
		Time average	Median value
D	0.0–3.5	80,000	58,000
	3.5–30.0	22,000	20,000
E	0.0–5.0	219,000	51,000
	5.0–30.0	37,000	17,000
F	0.0–3.0	74,000	46,000
	3.0–30.0	20,000	16,000

will be achieved at the leakage due to the critical condition of pressure difference). Hence, it can be said that an HTC value much higher than 26,000 $W/m^2/K$ will be achieved when the liquid sodium flow is dominant. At the same time, Yamaguchi *et al.* numerically suggested that the HTC in the SWR would be approximately 12,000 $W/m^2/K$ on a heat transfer outer tube surface under a gas-dominant condition (0.94 of void fraction).[7] Accordingly, the flow characteristics especially in terms of the void fraction could be discussed relatively based on the magnitude of the HTC. In the following discussion, the flow characteristics at each location have been investigated based on the transient history of the HTC.

(1) Initial Seconds of Injection

During the first several seconds of injection, the SWR jet is developing and covering up the measurement tube. Simultaneously, the liquid sodium on the tube is being swept out by the jet. Therefore, the HTC will increase due to the convection of liquid sodium and then fluctuate due to a multiphase effect. When a gas phase is dominant near the heat transfer tube, the HTC will decrease. At Location A (the lower side of the tube), it is determined that the HTC increases rapidly up to approximately 60,000 $W/m^2/K$ and then decreases to 20,000–30,000 $W/m^2/K$ approximately 2 s after the injection, as shown in Fig. 6. Hence, it could be said that the reacting gas covers up Location A at that time. On the other hand, an instantaneously high HTC is not calculated at Location C at the beginning of the injection, as shown in Fig. 9. The representative value is estimated to be 15,000 $W/m^2/K$ during the initial 8 s, which is almost consistent with that of the gas-dominant condition (12,000 $W/m^2/K$). Therefore, it might be said that the reacting gas instantaneously covers up Location C instantaneously (faster than Location A).

At the upper side, the comparatively high value of the HTC (> 100,000 $W/m^2/K$) and the wide fluctuation are noted during the initial 5 s regardless of the location (D–F), as shown in Figs. 10–12. The representative value is estimated to be approximately 50,000 $W/m^2/K$, which corresponds to that during the initial 2 s at Location A. Therefore, liquid sodium will be a dominant fluid and the influence of liquid sodium will be not negligible at the upper side during this period. A schematic of the fluid condition is illustrated in **Fig. 13**.

(2) 5 to 18 Seconds of Injection

At the lower side of the tube, the representative value

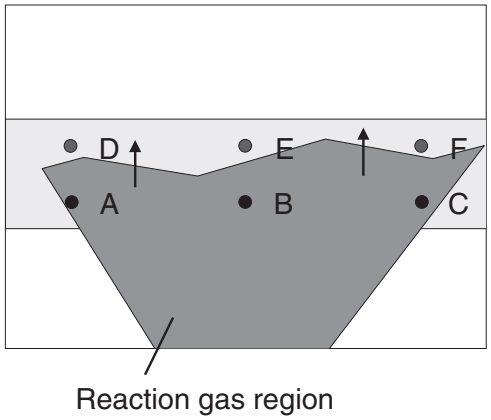

Fig. 13 Schematic of the gas region (0–5 s)

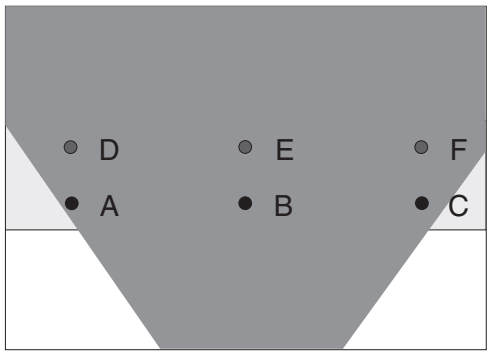

Fig. 14 Schematic of the gas region (5–18 s)

of the HTC remains comparatively small (25,000–42,000 $W/m^2/K$) during this period, as shown in Table 1. At the same time, the magnitude of the fluctuation increases gradually at both Locations A and C. Probably, the influence of liquid sodium affects the fluctuation. Comparison of Figs. 6 and 9 shows that the magnitude of the fluctuation is larger at Location A than at Location C. In general, a void fluctuation and a velocity fluctuation, which can cause the HTC fluctuation, become stronger at an interface of the jet. Hence, it might be concluded that the interface of the reacting jet exists near Location A rather than Location C.

At the upper side, the same tendency is obtained at each location (D, E, and F), as seen in Figs. 10–12. The representative value of the HTC is around 20,000 $W/m^2/K$, which is lower than the stagnant liquid sodium condition (26,000 $W/m^2/K$). Also, a fluctuation of small magnitude is obtained during this period. Consequently, it suggests that the upper side of the tube is consistently covered up with the gas phase. The reaction gas region during this period is illustrated in **Fig. 14**.

(3) 18 to 30 Seconds of Injection

As shown in Figs. 6 and 9 and Table 1, the quite large fluctuation and the high representative value (100,000 $W/m^2/K$) are obtained at the lower side of the tube (Locations A and C). Considering the wide range of the fluctuation, the interface of the reaction region will exist near Locations A and C during this period as well as the preceding period (5–18 s). On the other hand, the representative value is about three times as large as that in the preceding period (Table 1). Because a constant leakage rate (during the injection) was observed in the experiment,[3] it is difficult to explain the increase in the value following a velocity change. Therefore, it could be said that a liquid phase covers up Locations A and C and that the influence of liquid sodium increases significantly during this period.

Let us discuss the validity of the high HTC (>100,000 $W/m^2/K$) by assuming a liquid phase flow. For simplicity, the following Subbotin's heat transfer correlation[8] for liquid metal is applied using the tube outer diameter as a characteristic length.

$$Nu = 5 + 0.025Pe^{0.8}. \tag{4}$$

Here, Nu and Pe mean the Nusselt number and Peclet number, respectively. Nu and Pe are defined as

$$Nu = hL/\lambda, \tag{5}$$

$$Pe = PrRe = \nu/\alpha \times UL/\nu, \tag{6}$$

where L is the characteristic length. Pr and Re are the Prandtl number and Reynolds number, respectively. α is the thermal diffusivity. ν and U are the dynamic of viscosity and average velocity, respectively. From Eqs. (4) to (6), the average velocity is calculated as

$$U = \frac{\nu}{LPr}\left(\frac{hL/\lambda - 5}{0.025}\right)^{1.25}. \tag{7}$$

For the physical properties of liquid sodium at 1,100 K and $h = 113{,}000\,W/m^2/K$, the average velocity is estimated to be 31.1 m/s. In the benchmark analysis of SWAT-1R with a multidimensional and multiphase thermal hydraulics simulation,[9] the gas phase velocity was determined to be more than 100 m/s at the measurement tube. Therefore, it will be possible to achieve about 30 m/s for the liquid phase velocity near the interface of the reaction gas region.

Concerning the upper side of the tube (Locations D–F), the HTC does not change in comparison with the preceding period (5–18 s), as seen in Figs. 10–12. Hence, it is suggested that the upper side of the tube remains to be covered up by the gas phase during this period. **Figure 15** shows the schematic of the fluid condition during this period. As shown in Fig. 15, the gas region is estimated to spread out at the upper side of the tube. This might result from the collision of the gas region at the lower side of the tube.

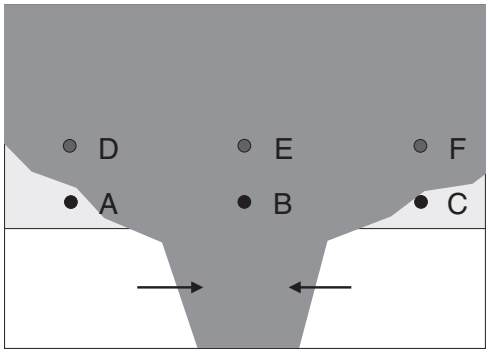

Fig. 15 Schematic of the gas region (18–30 s)

V. Conclusions

Numerical investigation of the transient behavior of the heat transfer coefficient (HTC) on the heat transfer tube under the sodium-water reaction (SWR) configuration region has been carried out in order to achieve a precise estimation of the HTC during the SWR. In the investigation, the temperature data obtained in the experiment (SWAT-1R) is used. A one-dimensional heat conduction equation in the cylindrical coordinate system is assumed inside the tube, while an overall HTC of homogeneous fluid is applied to the adjacent flow region. To estimate the HTC, the inverse problem approach is applied and the bisection method is used to calculate the HTC. As a result, it is concluded that the value of the HTC varies widely during the SWR, and that different transient behaviors are obtained between the upper and lower sides of the tube measurement. To determine the representative value of the HTC over some time periods that are selected based on the transient behavior, the time average and median values are examined. Since the time average value is much affected by an extremely large value calculated in the analysis, which was also reproduced in the experiment, the median value is adopted as the representative value in the present study.

The flow characteristics have also been investigated based on the analytical result in terms of void fraction. At the lower side of the measurement tube, the comparatively small value and small-scale fluctuation of the HTC are calculated for the first 5 s after injection. In one location (Location A), the HTC is fluctuated widely at the very beginning of the injection (0–2 s), which is caused by the sweep of liquid sodium. The average value is evaluated to be 15,000–34,000 $W/m^2/K$. Then, the average value and scale of the fluctuation increase gradually until approximately 18 s from the injection. After 18 s, the average value increases suddenly up to 113,000–128,000 $W/m^2/K$ and a large-scale fluctuation is obtained.

In contrast, the comparatively high average value of the HTC (46,000–58,000 $W/m^2/K$) is evaluated during the first 5 s at the upper side of the tube. In addition, the large-scale fluctuation, which will correspond to that obtained for the first 2 s at Location A, is calculated in the analysis. After 5 s from the injection, the average value is evaluated to be 16,000–20,000 $W/m^2/K$, and the range of the fluctuation becomes small.

In the present study, the flow characteristics have also been presumed based on the analysis in terms of the reaction gas region (void fraction). The overall HTC (26,000 $W/m^2/K$) in which only the thermal conductivity of liquid sodium is assumed and the numerical investigation of the previous work (12,000 $W/m^2/K$) under the gas-phase-dominant condition (0.94 of void fraction) are used as references. The experimental duration of the reaction gas region is illustrated at each time period. A numerical quantification of the correlation between the void fraction and the HTC is planned for a future study.

Nomenclature

A: cross-sectional area [m^2]
C_p: specific heat [J/kg/°C]
h: heat transfer coefficient [$W/m^2/K$]
L: characteristic length [m]
Nu: Nusselt number
Pe: Peclet number
Pr: Prandtl number
Re: Reynolds number
r: radial coordinate [m]
T: temperature [°C]
T_f: temperature of fluid [°C]
r_b: outer radius of tube [m]
T_F: temperature degrees Fahrenheit [°F]
t: time [s]
U: velocity of the fluid [m/s]
Greek Letters
α: thermal diffusivity [m^2/s]
Δt: time step [s]
ΔV: volume of the cell [m^3]
λ: thermal conductivity [W/m/K]
ν: dynamic coefficient of viscosity [m^2/s]
ρ: density [kg/m^3]
Subscripts/Superscripts
i: i-th control volume
$i \pm 1$: adjoining control volumes of i-th volume
$i \pm 1/2$: boundary between control volumes
0: temperature in the last time step

References

1) R. Currie, G. A. B. Linekar, D. M. Edge, "The under sodium leak in the PFR superheater 2 in February 1987," *Proc. Specialists' Meeting on Steam Generator Failure and Failure Propagation Experience*, Aix-en-Province, France, Sep. 26–28, 1990, 107–132 (1990).
2) O. Miyake, H. Hamada, H. Tanabe *et al.*, *The Development and Application of Overheating Failure Model of FBR Steam Generator Tubes (IV)*, JNC Technical Report, 16 (2004), [in Japanese].
3) M. Nishimura, K. Shimoyama, A. Kurihara, H. Seino, *Sodium-Water Reaction Test to Confirm Thermal Influence on Heat Transfer Tubes*, JNC Technical Report, TN9400-2003-014 (JNC) (2003), [in Japanese].
4) M. Hori, "Sodium/water reactions in steam generators of liquid metal fast breeder reactors," *At. Energ. Rev.*, **18**[3], 707–778 (1980).
5) H. Takasu, M. Isozaki, Y. Himeno, T. Iguchi, *Physical Properties for Sodium Technology (Na, Ar, He, 304SS, 316SS, 2-1/4Cr-1Mo)*, PNC N941 81 73 (PNC) (1981), [in Japanese].
6) C. F. Braum & Co., *Design Guide for LMFBR Sodium Piping*, Report No. SAN-78-1 (1971).
7) A. Yamaguchi, T. Takata, H. Ohshima, A. Kurihara, "Thermal influence on steam generator heat transfer tube during sodium-water reaction accident of sodium-cooled fast reactor," *Proc. NURETH12*, Pittsburgh, Pennsylvania, USA, Sep. 30–Oct. 4, 2007 (2007).
8) JSME, *JSME Data Book: Heat Transfer 4th Edition*, JSME, Japan, 106–107 (1986), [in Japanese].
9) T. Takata, A. Yamaguchi, "Numerical approach to the safety evaluation of sodium-water reaction," *J. Nucl. Sci. Technol.*, **40**[10], 708–718 (2003).